Current Biology 16, 1026–1033, May 23, 2006 ©2006 Elsevier Ltd All rights reserved DOI 10.1016/j.cub.2006.04.004

Report

# Modeling Clinically Heterogeneous Presenilin Mutations with Transgenic *Drosophila*

**Glen A. Seidner,[1,2,4] Yihong Ye,[4,5] Martha M. Faraday,[3] W. Gregory Alvord,[3] and Mark E. Fortini[1,4,*]**

[1] Laboratory of Protein Dynamics and Signaling
[2] Basic Research Program
SAIC-Frederick, Inc.
[3] Data Management Services
NCI-Frederick
National Institutes of Health
Frederick, Maryland 21702
[4] Department of Genetics
University of Pennsylvania School of Medicine
Philadelphia, Pennsylvania 19104
[5] Laboratory of Molecular Biology
NIDDK
National Institutes of Health
Bethesda, Maryland 20892

## Summary

**To assess the potential of *Drosophila* to analyze clinically graded aspects of human disease, we developed a transgenic fly model to characterize *Presenilin* (*PS*) gene mutations that cause early-onset familial Alzheimer's disease (FAD). FAD exhibits a wide range in severity defined by ages of onset from 24 to 65 years [1]. PS FAD mutants have been analyzed in mammalian cell culture, but conflicting data emerged concerning correlations between age of onset and PS biochemical activity [2–4]. Choosing from over 130 FAD mutations in *Presenilin-1*, we introduced 14 corresponding mutations at conserved residues in *Drosophila* Presenilin (Psn) and assessed their biological activity in transgenic flies by using genetic, molecular, and statistical methods. Psn FAD mutant activities were tightly linked to their age-of-onset values, providing evidence that disease severity in humans primarily reflects differences in PS mutant lesions rather than contributions from unlinked genetic or environmental modifiers. Our study establishes a precedent for using transgenic *Drosophila* to study clinical heterogeneity in human disease.**

## Results and Discussion

Presenilin is an evolutionarily conserved polytopic membrane protein that is part of the multisubunit γ-secretase complex responsible for intramembranous cleavage of several transmembrane proteins, including APP, Notch, Delta, DCC, ErbB4, N-Cadherin, and E-Cadherin [5]. Familial Alzheimer's disease (FAD) mutations in *Presenilin-1* (*PS1*) and *PS2* alter proteolytic processing of APP to generate more toxic Aβ42 peptides that accelerate amyloid plaque formation in brain tissues [6]. PS mutations also contribute to neurodegeneration and cognitive decline through amyloid-independent mechanisms [7], involving altered regulation of receptor signaling and intracellular kinase pathways [7–10].

The *Drosophila APP* ortholog, *APPL*, lacks homology to APP within the Aβ peptide region, and loss of *APPL* produces subtle behavioral deficits that are difficult to measure quantitatively [11]. A more suitable substrate to monitor Presenilin (Psn) FAD mutant activity in *Drosophila* is the Notch receptor, the most extensively characterized fly γ-secretase substrate. Psn is required throughout *Drosophila* development for Notch signaling, and a wide variety of Notch-related phenotypes exist that range from severe embryonic lethality to specific defects in adult tissues. This phenotypic range is amenable to characterizing variable degrees of function among different Psn FAD mutants. In addition, genetic and molecular reagents are available to characterize Notch biochemical cleavage and subsequent target-gene activation in *Drosophila*.

Previous studies have successfully used transgenic mice and *C. elegans* to assess the genetic properties of human PS FAD mutants [12–15], and one study suggested a potential difference between two FAD variants [14]. However, quantitative comparison between FAD mutants was not practical because of heterologous expression methods and difficulties controlling transgene copy numbers. Two studies in mammalian cell culture showed little or no relationship between average ages of onset and Aβ42 secretion levels [3, 4], contrary to one study reporting a strong correlation [2].

We assessed PS FAD mutant function in *Drosophila* by expressing 14 FAD-linked mutant *psn* transgenes in animals lacking endogenous *psn* function. The mutations were selected on the basis of the following criteria: (1) they span the entire protein (Figure 1A), (2) relatively large numbers of families and affected individuals have been identified for most mutations (Figure 1B), and (3) their ages of onset range from 24 to 65 years, or are possibly asymptomatic (E318G and F175S; Figure 1B) [16–19]. Thirteen of the mutations affect residues that are conserved in fly Psn, and the remaining one alters a conservatively substituted residue (Figure 1A). To achieve physiological expression of the transgenes, we defined a 1.5 kb promoter, termed *PEPC* (*P*resenilin *e*ndogenous *p*romoter *c*assette), of the endogenous *psn* gene. At the larval-pupal transition, loss of *psn* function causes highly uniform lethality that is fully rescued by a wild-type *PEPC-psn* transgene but not by wild-type human *PS1* or *PS2* transgenes driven by *PEPC* (data not shown). To circumvent this technical problem with human *PS* transgenes, we engineered each FAD mutation into the fly *psn* gene.

Examining transgenic lines expressing *PEPC-psn* FAD mutants in a *psn* null genetic background, we defined eight distinct phenotypic categories that represent a graded series in order of increasing rescue ability, as follows: (1) prepupal lethal, (2) late prepupal lethal, (3) pupal lethal, (4) pharate lethal, (5) severe neurogenic/adult

*Correspondence: fortini@ncifcrf.gov

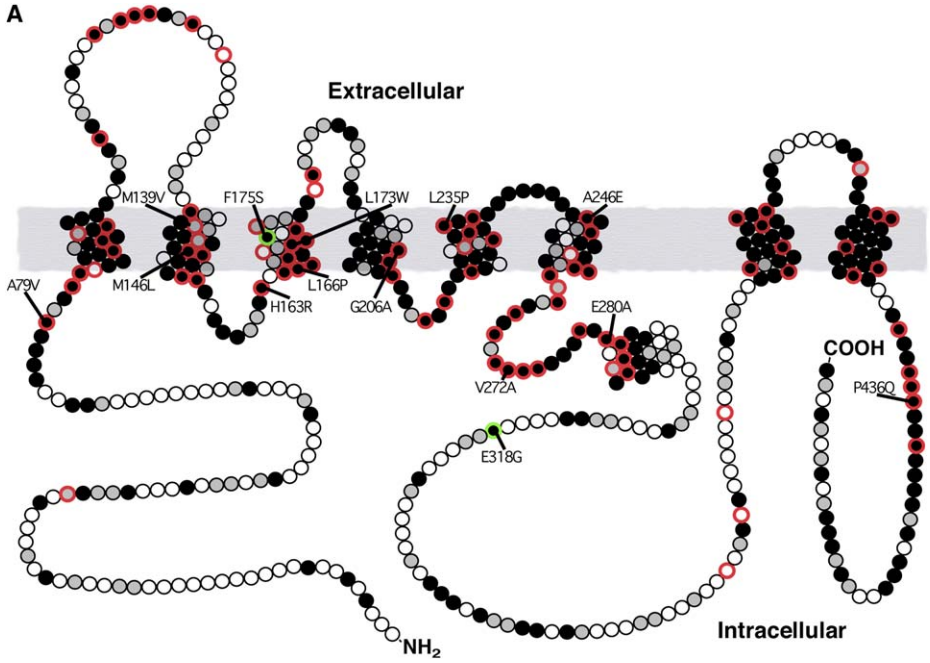


B

| FAD Mutation | Average Age of Onset | # of Fam (Pat) |
|---|---|---|
| L166P | 24.0 | 1(1) |
| L173W | 26.5 | 1(2) |
| P436Q | 28.3 | 3(5) |
| V272A | 31.8 | 1(4) |
| L235P | 32.3 | 2(6) |
| M146L | 39.8 | 6(8) |
| M139V | 40.7 | 8(23) |
| H163R | 46.1 | 10(45) |
| E280A | 47.4 | 12(112) |
| A246E | 52.5 | 2(4) |
| G206A | 54.2 | 9(24) |
| A79V | 61.1 | 4(15) |
| E318G | No Ph. | 23(24) |
| F175S | No Ph. | 1(3) |

Figure 1. FAD-Associated Mutants in PS1 Selected for Analysis in Transgenic *Drosophila*

(A) Diagram of human PS1 indicating the 14 FAD-associated missense mutations that were engineered into *Drosophila* Psn. Solid, shaded, and open circles represent identical, similar, and nonconserved amino acids, respectively, between human and *Drosophila* Presenilins. Red and green circle borders indicate sites of pathogenic and nonpathogenic substitutions, respectively.

(B) FAD mutant average ages of onset (AAO), the number of affected families (# of Fam), and total number of affected patients (Pat). AAO values for the asymptomatic variants E318G and F175S are given as "no phenotype" (No Ph.) [19].

lethal, (6) moderate neurogenic/adult viable, (7) weak neurogenic/adult viable, and (8) morphologically normal (Figure 2). Quantitative analysis of survival rates, incidence of dorsoscutellar bristle duplications, wing notching, wing vein defects, and other morphological features was performed to assign each transgenic line to the appropriate rescue category (see Table S1 in the Supplemental Data online for details of quantitative scoring).

The phenotypic categories are consistent with an ordered series attributable to progressive increases in Psn-dependent Notch activation, but it was important to verify that they do not instead represent the effects of Psn on other substrates. In the canonical Notch pathway, ligand binding to the Notch receptor leads to ectodomain removal and subsequent γ-secretase-mediated intramembranous cleavage of Notch [20]. The liberated intracellular domain, termed NICD, translocates to the nucleus and participates directly in transcriptional regulation of target genes, including the *Enhancer of split m7* (*E(spl)m7*) gene in *Drosophila* [21]. Activation of Notch signaling within proneural cell clusters destined to give rise to adult sensory organs results in restricted expression of the proneural marker *scabrous (sca)* [22]. Visualization of *sca* expression in the larval imaginal wing disc with a *sca-lacZ* transgene provides evidence for a progressive range of Notch signaling with different *PEPC-psn* transgenes (Figures 2E–2H).

Biochemical evidence for progressively increasing Psn function was obtained by immunoblot analysis of Notch cleavage products across the spectrum of *PEPC-psn* FAD phenotypes (Figure 3). Representative PEPC-FAD transgenic lines of the different categories exhibit partial-to-complete failure in γ-secretase-mediated NICD production. Interestingly, although transgenic lines belonging to categories 2–4 exhibit significant levels of biological rescue activity, they do not produce levels of NICD detectable by immunoblot analysis. These results demonstrate that genetic assays such as ours are valuable for studying low-level or tissue-specific aspects of γ-secretase substrate cleavage that might not be amenable to biochemical analysis.

To determine whether the *PEPC-psn* FAD phenotypic series is similarly correlated with Notch target-gene activation, we used semiquantitative RT-PCR to monitor activation of the *E(spl)m7* gene (Figure 4). Normalizing transcriptional activation to two control genes, we observed a progressive increase in *E(spl)m7* transcript levels across categories 1–8, confirming that they represent graded increases in γ-secretase-dependent Notch activation. To verify this relationship, we utilized a temperature-sensitive *Notch* allele termed $N^{ts1}$. Incremental levels of Notch activity obtained by raising $N^{ts1}$ flies at different temperatures produced phenotypes matching those seen in the Psn FAD mutant series, but were independent of manipulations involving endogenous or transgenic Psn. Levels of *E(spl)m7* transcriptional activation seen in these $N^{ts1}$ phenotypic classes resembled closely those observed in the corresponding *PEPC-psn* FAD classes, confirming the progressive increase in Notch target-gene activation across this phenotypic spectrum (Figure 4). Taken together, these results validate the use of our phenotypic criteria to characterize varying degrees of *PEPC-psn* FAD transgene activity toward the endogenous γ-secretase substrate Notch.

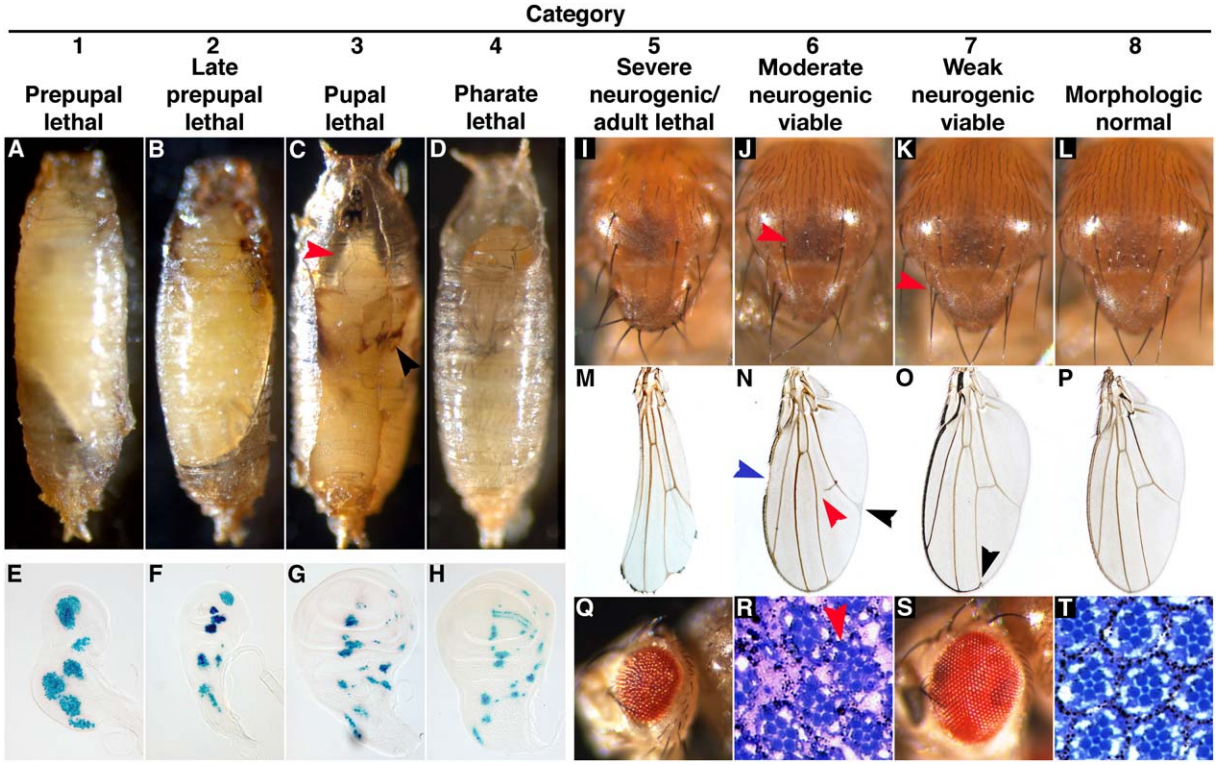


Figure 2. Representative Phenotypes Used to Assess Functional Rescue Activity of Psn FAD Mutants in Transgenic *Drosophila*

(A–H) Adult-lethal categories 1–4 exhibit progressively later lethality and increased morphological rescue during pupal stages ([A–D]; red arrowhead, rudimentary head structure; black arrowhead, early leg structures in [C]) and progressively more normal proneural cluster patterning as visualized by *sca-lacZ* labeling [24, 25] (E–H).

(I–P) Increasingly normal thoracic bristle patterning (I–L) and more complete wing development (M and N) across adult-viable categories 5–8 as indicated at top (red arrowhead in [K], duplicated dorsocutellar macrochaete; red arrowhead in [J], patch of missing microchaetae; blue arrowhead in [N], mild wing notching; black arrowheads in [N] and [O], wing vein deltas; and red arrowhead in [N], wing vein gap).

(Q–T) Small, roughened eye phenotype of a category 5 adult (Q) containing supernumerary photoreceptor cells ([R], red arrowhead) as compared to a fully rescued category 8 wild-type Psn transgenic adult retina (S and T). For phenotypic classification, single-copy *PEPC-psn* transgenes were introduced into flies lacking endogenous *psn* function and scored with several quantitative measures, as described in Table S1. Anterior is at top ([A–D] and [I–L]), right (E–H), and left ([M–Q] and [S]).

A limitation of transgenic analysis in *Drosophila* is that the transgenes are inserted at essentially random genomic locations, leading to variations in expression as a result of local position effects at different sites. These effects are a confounding factor in our comparisons of relative degrees of rescue function, which reflects properties of the primary lesion in each Psn mutant protein as well as the expression level of each transgenic insertion. We therefore generated from four to 16 independent insertions for each transgene, and each insertion was scored with multiple quantitative morphological criteria and assigned to the appropriate phenotypic category (see above and Table S1). The resulting data for all 162 transgenic lines, representing 14 *PEPC-psn* FAD mutants and one wild-type Psn control construct, are graphically presented in Figure 5A. Visual inspection suggests a positive overall trend between increasing age of onset in human FAD pedigrees and increasing

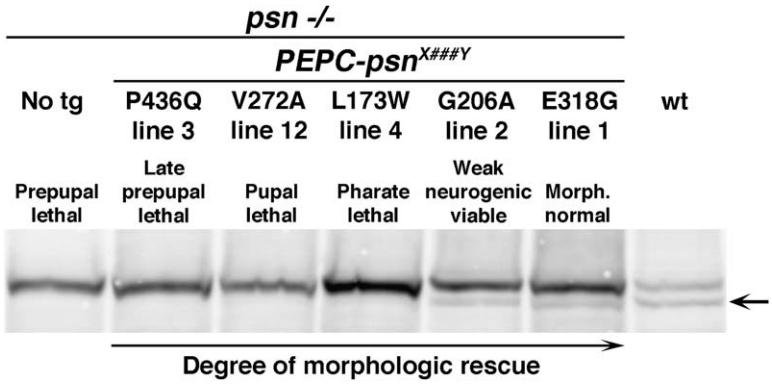


Figure 3. Levels of Notch Intramembrane Proteolysis in Psn FAD Mutant Transgenic Flies

Notch-activation results in ectodomain removal and generation of membrane-anchored C-terminal NEXT (upper band), which is cleaved intramembranously by γ-secretase to produce NICD (lower band; arrow at right). Nontransgenic *psn* null mutant larvae fail to produce detectable NICD from NEXT (leftmost lane). Transgenic lines bearing different Psn FAD transgenes in this *psn* null background exhibit increasing NICD levels that correlate with their degree of morphological rescue, as noted above each lane (No tg denotes no transgene; wt denotes wild-type).

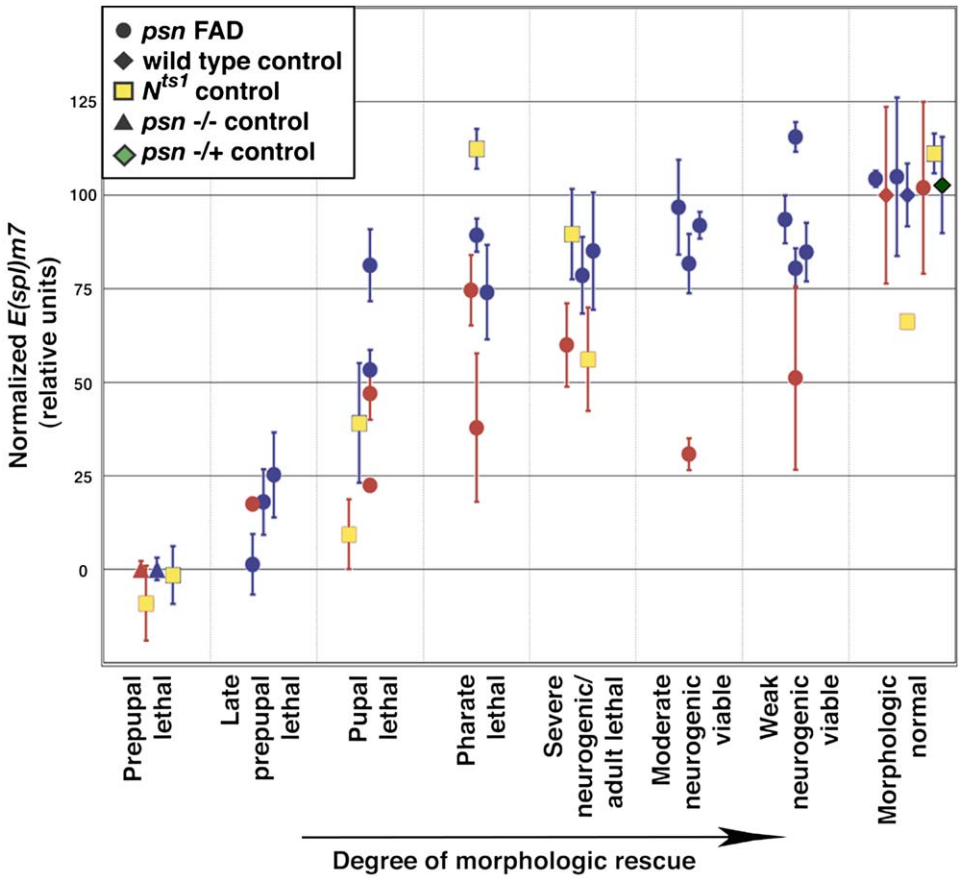


Figure 4. Psn FAD Transgenic Flies Exhibit a Graded Range of *E(spl)m7* Transcriptional Activation Correlated to Their Notch Signaling Phenotypes

Transcriptional activation of the Notch target gene *E(spl)m7* (y axis) was monitored by RT-PCR across a representative sampling of Psn FAD transgenic lines covering the eight morphological categories (x axis). *E(spl)m7* transcript levels were normalized to levels of *Notch* mRNA, because Notch signaling is sensitive to receptor dosage [26] and *Notch* transcription might thus be susceptible to perturbations in Psn activity. We confirmed RT-PCR results of *E(spl)m7* normalized to *Notch* (blue symbols) with an independent RT-PCR using ribosomal-protein gene *Rp49* (red symbols) for normalization. RT-PCR ratios for transgenic lines bearing a single-copy *PEPC-psn* FAD construct in a *psn* null background are indicated as circles; control genotypes are as follows: wild-type (red and blue diamonds), $N^{ts1}$ flies raised at different temperatures (yellow squares), *psn* homozygote null (red and blue triangles), and *psn* heterozygotes (green diamond). Error bars represent ± standard error of the mean.

biological activity for these FAD mutants in transgenic *Drosophila*.

To investigate this potential trend, we applied a number of statistical tests to the transgenic scoring data. We used exclusively nonparametric tests that treat the data only as ordinally ranked categories. This conservative approach was used because age-of-onset figures are derived from relatively small human sample sizes, and we cannot affix quantitative values to the eight phenotypic rescue categories, although we are confident of their progressive ordinal ranking. The Jonckheere-Terpstra test [23] for ordered alternatives is a nonparametric test that fits these assumptions. For this analysis, the very-late-onset/probable asymptomatic mutants F175S and E318G were placed in a single group ordered prior to the wild-type Psn transgene. Using this test, we find a highly significant correlation between the age-of-onset ranking of the FAD mutants and the relative biological activities of the corresponding Psn mutant transgenes ($p < 0.0001$; J-T statistic = 6.9). We also analyzed the data with Spearman's rho [23], a nonparametric test for correlation between two variables without the assumption of a linear relationship, which similarly demonstrates a highly significant correlation between age-of-onset values and biological activities in *Drosophila* ($p < 0.0001$; correlation = +0.531).

The above tests demonstrate an overall correlation across the dataset as a whole, but Figure 5A indicates that the correlation is not smooth. Most FAD mutants appear to cluster in groups separated by discontinuities, with a few mutants that are noticeably different from nearby mutants. To investigate these features, we performed pairwise rank-sum comparisons between all individual Psn FAD mutants with the Wilcoxon-Mann-Whitney test, a nonparametric method for analyzing the overlap between distributions of two independent groups [23]. We found that mutants having similar ages of onset are, in general, not statistically different from one another (Figure 5B). Nevertheless, the mutants can be statistically grouped into three distinct classes: strong (L166P, L173W, P436Q, V272A, and L235P; Figures 5C and 5D), intermediate (M146L, M139V, H163R,

A

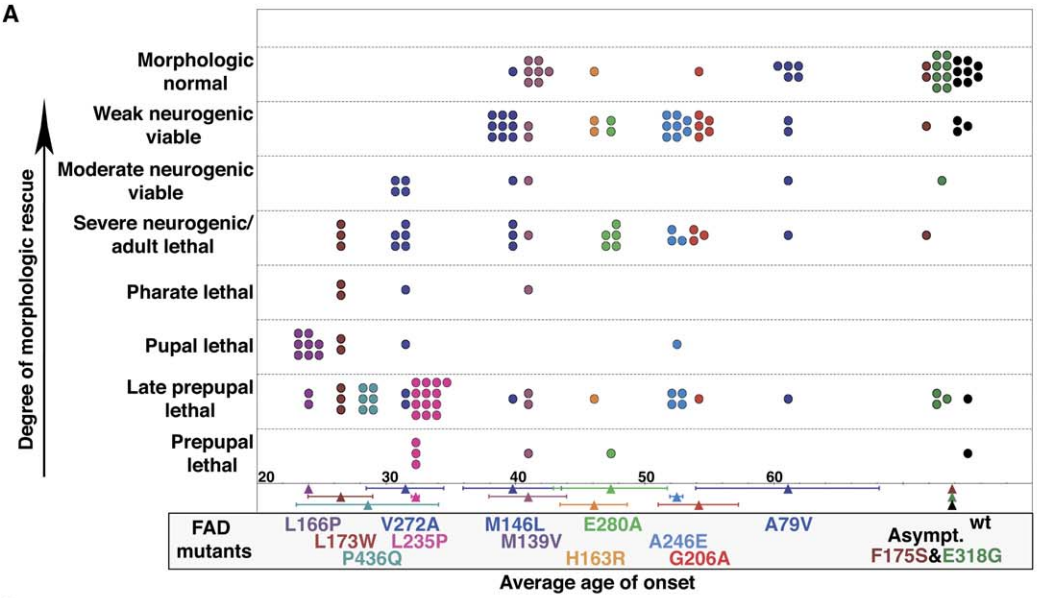


B

P values for pairwise comparisons between mutants (Wilcoxon-Mann-Whitney test)

| Ordinal rank/ mutant | 1 (L166P) | 2 (L173W) | 3 (P436Q) | 4 (V272A) | 5 (L235P) | 6 (M146L) | 7 (M139V) | 8 (H163R) | 9 (E280A) | 10 (A246E) | 11 (G206A) | 12 (A79V) | 13 (F175S, E318G) | 14 (Dm+14) |
|---|---|---|---|---|---|---|---|---|---|---|---|---|---|---|
| 1 (L166P) | | 0.2207 | 0.0027* | 0.0055 | 0.000063* | 0.00014 | 0.0072 | 0.0828 | 0.0047 | 0.0277 | 0.0012 | 0.0012 | 0.0034 | 0.0028 |
| 2 (L173W) | | | 0.0116* | 0.051 | 0.00026* | 0.00066 | 0.0164 | 0.0974 | 0.0357 | 0.0534 | 0.0041 | 0.0021 | 0.0037 | 0.0031 |
| 3 (P436Q) | | | | 0.0023 | 0.2648 | 0.00051 | 0.007 | 0.0177 | 0.0131 | 0.0041 | 0.0018 | 0.0019 | 0.0017 | 0.0049 |
| 4 (V272A) | | | | | 0.000016* | 0.0038 | 0.046 | 0.1052 | 0.6168 | 0.2414 | 0.0323 | 0.0049 | 0.0071 | 0.0018 |
| 5 (L235P) | | | | | | 0.0000018 | 0.000092 | 0.0029 | 0.00087 | 0.000025 | 0.000022 | 0.000023 | 0.0000086 | 0.00009 |
| 6 (M146L) | | | | | | | 0.4389 | 0.6556 | 0.0709 | 0.1644 | 0.8299 | 0.1519 | 0.0729 | 0.0203 |
| 7 (M139V) | | | | | | | | 0.7937 | 0.1275 | 0.1085 | 0.4572 | 0.616 | 0.4349 | 0.3656 |
| 8 (H163R) | | | | | | | | | 0.2089 | 0.3076 | 0.648 | 0.5507 | 0.3763 | 0.29 |
| 9 (E280A) | | | | | | | | | | 0.6259 | 0.1636 | 0.0242 | 0.0226 | 0.0091 |
| 10 (A246E) | | | | | | | | | | | 0.319 | 0.0266 | 0.012 | 0.0046 |
| 11 (G206A) | | | | | | | | | | | | 0.1686 | 0.1024 | 0.0423 |
| 12 (A79V) | | | | | | | | | | | | | 0.7913 | 0.6052 |
| 13 (F175S, E318G) | | | | | | | | | | | | | | 0.9197 |
| 14 (Dm+14) | | | | | | | | | | | | | | |

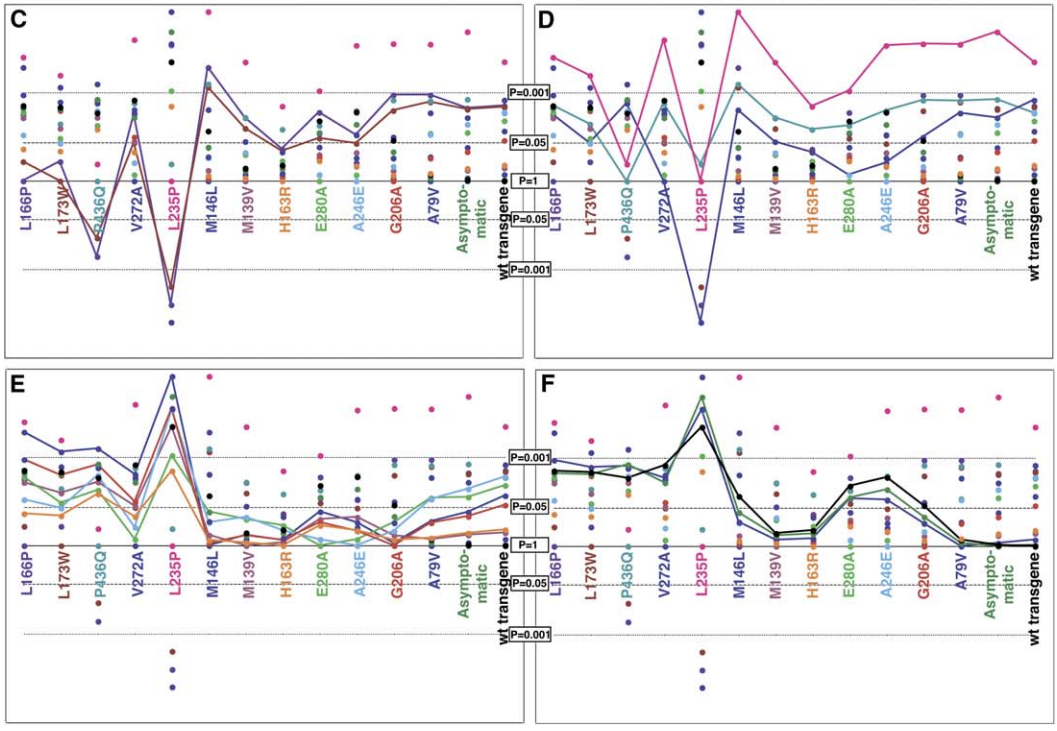

E280A, A246E, and G206A; Figure 5E), and weak (A79V, F175S, and E318G; Figure 5F). Strong mutants differ most clearly from the weak ones in terms of function (Figures 5C and 5D), and vice versa (Figure 5F), whereas the intermediate group shows more modest differences compared to either of these two flanking groups (Figure 5E). Pairwise comparisons of aggregated mutant groups confirmed these classes. The strong mutant group is significantly different from both the intermediate and weak groups ($p < 0.0001$ in both cases). Despite its age of onset of ~60, the A79V mutant is more similar to the weak mutants than the intermediate ones, as confirmed by pairwise comparisons of aggregated intermediate and weak groups with A79V assigned to either the intermediate ($p = 0.0027$) or the weak group ($p = 0.00049$).

Similarly, two mutants, L235P and P436Q, are less functional in transgenic flies than might be predicted on the basis of their ages of onset, whereas another mutant, M139V, is somewhat more functional than expected. Whether these disparities reflect inadequate age-of-onset data, modifier effects in the corresponding human pedigrees, or an unknown feature of the fly assay system is not clear. Finally, the E318G and F175S mutants, proposed to be either very weak pathogenic mutants or functionally normal polymorphisms, are statistically indistinguishable from the wild-type transgene in our genetic assay, consistent with the idea that they are nonpathogenic polymorphisms. Overall, our results support the assertion that disease severity in early-onset Alzheimer's disease is primarily determined by PS mutant lesion type as opposed to unlinked genetic or environmental modifiers, as was also deduced from a study of Aβ secretion levels in PS FAD mutant transfected cells [2].

A few other interesting patterns emerge from these comparisons. Mutants for which relatively few independent lines were obtained, most notably H163R ($n = 4$), fail to show significant differences when compared to other mutant groups (Figures 5C–5F). On the basis of the complete dataset, we estimate that ~10 independent lines of a given mutant are required to obtain statistically useful data. This problem might be circumvented by employing a "knock in" strategy to precisely replace the endogenous *psn* gene with FAD variants, an approach that is not yet reliable in *Drosophila*. Additionally, one source of experimental noise is that transgenes occasionally insert into locations where they are poorly expressed or damaged during insertion, as is evident from a few instances involving the "asymptomatic" F175S and E318G mutant and wild-type transgenes. Normalization of functional read-outs for each transgene insertion relative to its mRNA or protein expression level in the appropriate transcript null or protein null *psn* mutant background should reduce this noise and lead to further refinement of the statistical data.

Our findings establish the validity of using transgenic *Drosophila* or other heterologous organisms to evaluate clinically heterogeneous aspects of human diseases with a clearly defined genetic etiology. Transgenic *Drosophila* offer several advantages to augment more traditional clinical assessments as well as transgenic mouse models. Transgenic flies are relatively inexpensive and rapid to produce, large numbers of independent lines can be easily generated, and limitless numbers of progeny for each line can be examined under controlled genetic conditions. These features of our assay might make it useful for obtaining a rapid estimate of approximate disease severity for new *PS1* and *PS2* mutations, especially for those with limited pedigree data, small numbers of affected individuals, or suspected environmental or genetic confounding factors. Although the primary goal of this study was to assess an array of genetically diverse FAD mutant variants in a more standardized genetic background, the transgenic flies we characterized could be used to study the effects of suspected modifiers or search for new modifiers of PS function. The transgenic lines could also be combined with APP-expressing transgenes to investigate more directly the role of PS FAD mutants in APP cleavage, amyloid-peptide accumulation, and neurotoxicity in a fly model. The correlation we observe between the effects of different FAD mutations on *Drosophila* Notch signaling and human disease onset underscores recent proposals that in addition to APP processing, more global perturbations in pathways involving other γ-secretase substrates should be considered in early-onset Alzheimer's disease [7–10]. Finally, our results offer encouragement that additional transgenic *Drosophila* models might be developed to investigate clinical heterogeneity in other human diseases.

## Experimental Procedures

### FAD-Linked *PEPC-psn* Mutant Transgenes

Psn FAD transgenes generated by overlapping PCR were shuttled into the vector pCaSpeR containing a *Drosophila* wild-type *psn* cDNA backbone driven by the 1.5 kb *psn* promoter (*PEPC*), and missense mutation regions were sequenced. Transgenic animals were generated by embryo injection, and additional lines were produced

Figure 5. Correlation between Presenilin FAD Mutant Age of Onset in Human Pedigrees and Functional Activity in Transgenic *Drosophila*

(A) Morphological scoring of Psn FAD mutant transgenic lines. Each point represents an individual independent *PEPC-psn* FAD transgenic line, with color denoting each FAD mutant amino acid substitution positioned on the x axis according to increasing age of onset in years (error bars represent ± average deviation of the mean). The y axis represents the assignment of each transgenic line to one of the morphological categories at left, reflecting increasing transgene function (see Table S1 for quantitative scoring). Equivalent points have been evenly dispersed for clarity (wt denotes wild-type transgene).

(B) P values for pairwise Wilcoxon-Mann-Whitney tests. Each box shows the p value for one test performed between the corresponding FAD mutants shown at left and at top. P values <0.001 level are in yellow, those between 0.05 and 0.001 are in blue, and those that do not reach statistical significance are in white; asterisks indicate significant p values with an unexpectedly negative correlation between age of onset and relative transgenic activity.

(C–F) Plots of pairwise Wilcoxon-Mann-Whitney p values. Each plot shows the p values for all pairwise comparisons, with the 14 Psn FAD mutants and wild-type control arranged ordinally by age of onset and color-coded along the x axis, and with the negative log of the p value plotted on the y axis. Color coding of p values and connecting lines identifies the mutant group being compared to all the other mutants across the plot. For clarity, pairwise data are shown for Psn FAD mutant subsets in different plots as follows: (C) L166P and L173W; (D) P436Q, V272A, and L235P; (E) M146L, M139V, H163R, E280A, A246E, and G206A; and (F) A79V, F175S, E318G, and wild-type (F175S and E318G are grouped as "asymptomatic").

by mobilization with Δ2-3 transposase. Both wild-type splice-variant cDNAs rescued *psn* null animals with no distinguishable difference (data not shown), so all FAD variant transgenes were made with the longer splicing variant.

### Notch immunoblot analysis

Crosses were performed to generate larvae bearing a single-copy Psn FAD transgene (*PEPC-psn*$^{X\#\#\#Y}$) in a *psn*$^{B3}$ null background, and third-instar-larval brain-disc complexes were harvested and lysed in hypotonic buffer as described [24]. Total lysates were sonicated, and 40 μg of total protein per sample was resolved on a Bio-Rad Criterion XT 3%–8% Tris-Acetate gel, transferred to nitrocellulose, and probed with mouse anti-Notch 9C6 antibody (1:1000 dilution) recognizing the Notch intracellular domain (University of Iowa Developmental Studies Hybridoma Bank), followed by HRP-conjugated goat anti-mouse antibody (1:5000 dilution; Jackson Immunoresearch).

### *E(spl)m7* Semiquantitative RT-PCR

Duplex PCR was performed with four concentrations of a 2-fold titration of first-strand synthesis from third-instar-larval total RNA. PCR products were visualized by SyberGreen (Molecular Dynamics) staining and quantitated with Fuji ImageQuant software, and relative absorbance units were plotted against template concentration. Slopes best fitting a straight line ($R^2 \geq 0.95$) were taken as the rate proportional to transcript levels. *E(spl)m7* rates were normalized to similarly derived values for either *Notch* or *Rp49*, and final normalized data were graphed by setting *psn* null and wild-type control values at 0% and 100%, respectively. Data represent at least three independent PCR reactions with at least two replicated total-RNA preparations per sample (except "severe neurogenic/adult lethal" *Rp49* normalized samples, n = 2). *N*$^{ts1}$ animals were grown in continuous culture at five temperature increments between the permissive (19°C) and restrictive conditions (31°C), then harvested for RT-PCR or allowed to develop for phenotypic scoring. RT-PCR primer sequences are given in Table S2.

### Supplemental Data

Supplemental Data include two tables and are available with this article online at: http://www.current-biology.com/cgi/content/full/16/10/1026/DC1/.

### Acknowledgments

We thank Jairaj Acharya, Morris Birnbaum, Han Cho, Deborah Morrison, and lab members for helpful comments. This research was supported in part by the Intramural Research Program of the National Institutes of Health (NIH), National Cancer Institute, Center for Cancer Research, and with Federal funds under DHHS#NO1-CO-12400. Support was also provided by NIH grant AG14583 from the National Institute on Aging. The content of this publication does not necessarily reflect the views or policies of the Department of Health and Human Services, nor does mention of trade names, commercial products, or organizations imply endorsement by the U.S. government.

Received: February 16, 2006
Revised: March 29, 2006
Accepted: March 30, 2006
Published: May 22, 2006

### References

1. Larner, A.J., and Doran, M. (2006). Clinical phenotypic heterogeneity of Alzheimer's disease associated with mutations of the presenilin-1 gene. J. Neurol. *253*, 139–158.
2. Duering, M., Grimm, M.O., Grimm, H.S., Schröder, J., and Hartmann, T. (2005). Mean age of onset in familial Alzheimer's disease is determined by amyloid beta 42. Neurobiol. Aging *26*, 785–788.
3. Mehta, N.D., Refolo, L.M., Eckman, C., Sanders, S., Yager, D., Perez-Tur, J., Younkin, S., Duff, K., Hardy, J., and Hutton, M. (1998). Increased Aβ42(43) from cell lines expressing presenilin 1 mutations. Ann. Neurol. *43*, 256–258.
4. Murayama, O., Tomita, T., Nihonmatsu, N., Murayama, M., Sun, X., Honda, T., Iwatsubo, T., and Takashima, A. (1999). Enhancement of amyloidß42 secretion by 28 different presenilin 1 mutations of familial Alzheimer's disease. Neurosci. Lett. *265*, 61–63.
5. Brunkan, A.L., and Goate, A.M. (2005). Presenilin function and γ-secretase activity. J. Neurochem. *93*, 769–792.
6. Selkoe, D.J. (1998). The cell biology of β-amyloid precursor protein and presenilin in Alzheimer's disease. Trends Cell Biol. *8*, 447–453.
7. Saura, C.A., Choi, S.Y., Beglopoulos, V., Malkani, S., Zhang, D., Shankaranarayana Rao, B.S., Chattarji, S., Kelleher, R.J., 3rd, Kandel, E.R., Duff, K., et al. (2004). Loss of presenilin function causes impairments of memory and synaptic plasticity followed by age-dependent neurodegeneration. Neuron *42*, 23–36.
8. Baki, L., Shioi, J., Wen, P., Shao, Z., Schwarzman, A., Gama-Sosa, M., Neve, R., and Robakis, N.K. (2004). PS1 activates PI3K thus inhibiting GSK-3 activity and tau overphosphorylation: Effects of FAD mutations. EMBO J. *23*, 2586–2596.
9. Marambaud, P., Wen, P.H., Dutt, A., Shioi, J., Takashima, A., Siman, R., and Robakis, N.K. (2003). A CBP binding transcriptional repressor produced by the PS1/γ-cleavage of N-cadherin is inhibited by PS1 FAD mutations. Cell *114*, 635–645.
10. Marambaud, P., and Robakis, N.K. (2005). Genetic and molecular aspects of Alzheimer's disease shed light on new mechanisms of transcriptional regulation. Genes Brain Behav. *4*, 134–146.
11. Luo, L., Tully, T., and White, K. (1992). Human amyloid precursor protein ameliorates behavioral deficit of flies deleted for *Appl* gene. Neuron *9*, 595–605.
12. Baumeister, R., Leimer, U., Zweckbronner, I., Jakubek, C., Grunberg, J., and Haass, C. (1997). Human presenilin-1, but not familial Alzheimer's disease (FAD) mutants, facilitate *Caenorhabditis elegans* Notch signalling independently of proteolytic processing. Genes Funct. *1*, 149–159.
13. Davis, J.A., Naruse, S., Chen, H., Eckman, C., Younkin, S., Price, D.L., Borchelt, D.R., Sisodia, S.S., and Wong, P.C. (1998). An Alzheimer's disease-linked PS1 variant rescues the developmental abnormalities of *PS1*-deficient embryos. Neuron *20*, 603–609.
14. Levitan, D., Doyle, T.G., Brousseau, D., Lee, M.K., Thinakaran, G., Slunt, H.H., Sisodia, S.S., and Greenwald, I. (1996). Assessment of normal and mutant human presenilin function in *Caenorhabditis elegans*. Proc. Natl. Acad. Sci. USA *93*, 14940–14944.
15. Qian, S., Jiang, P., Guan, X.M., Singh, G., Trumbauer, M.E., Yu, H., Chen, H.Y., Van de Ploeg, L.H., and Zheng, H. (1998). Mutant human Presenilin 1 protects *presenilin 1* null mouse against embryonic lethality and elevates Aβ1–42/43 expression. Neuron *20*, 611–617.
16. Colacicco, A.M., Panza, F., Basile, A.M., Solfrizzi, V., Capurso, C., D'Introno, A., Torres, F., Capurso, S., Cozza, S., Flora, R., et al. (2002). F175S change and a novel polymorphism in presenilin-1 gene in late-onset familial Alzheimer's disease. Eur. Neurol. *47*, 209–213.
17. Goldman, J.S., Johnson, J.K., McElligott, K., Suchowersky, O., Miller, B.L., and Van Deerlin, V.M. (2005). Presenilin 1 Glu318Gly polymorphism: Interpret with caution. Arch. Neurol. *62*, 1624–1627.
18. Dermaut, B., Cruts, M., Slooter, A.J., Van Gestel, S., De Jonghe, C., Vanderstichele, H., Vanmechelen, E., Breteler, M.M., Hofman, A., van Duijn, C.M., et al. (1999). The Glu318Gly substitution in presenilin 1 is not causally related to Alzheimer disease. Am. J. Hum. Genet. *64*, 290–292.
19. Cruts, M., and Rademakers, R. (2006). Alzheimer Disease & Frontotemporal Dementia Mutation Database (http://www.molgen.ua.ac.be/ADMutations/default.cfm?MT=0&ML=0&Page=Home).
20. Wolfe, M.S., and Kopan, R. (2004). Intramembrane proteolysis: Theme and variations. Science *305*, 1119–1123.
21. Klämbt, C., Knust, E., Tietze, K., and Campos-Ortega, J.A. (1989). Closely related transcripts encoded by the neurogenic gene complex Enhancer of split of *Drosophila melanogaster*. EMBO J. *8*, 203–210.
22. Singson, A., Leviten, M.W., Bang, A.G., Hua, X.H., and Posakony, J.W. (1994). Direct downstream targets of proneural

activators in the imaginal disc include genes involved in lateral inhibitory signaling. Genes Dev. *8*, 2058–2071.
23. Siegel, S., and Castellan, N.J., Jr. (1988). Nonparametric statistics for the behavioral sciences, 2nd Edition (Boston, MA: McGraw-Hill).
24. Ye, Y., Lukinova, N., and Fortini, M.E. (1999). Neurogenic phenotypes and altered Notch processing in *Drosophila Presenilin* mutants. Nature *398*, 525–529.
25. Struhl, G., and Greenwald, I. (1999). Presenilin is required for activity and nuclear access of Notch in *Drosophila*. Nature *398*, 522–525.
26. Artavanis-Tsakonas, S., Rand, M.D., and Lake, R.J. (1999). Notch signaling: Cell fate control and signal integration in development. Science *284*, 770–776.